Journal of Building Pathology and Rehabilitation (2022) 7:84
https://doi.org/10.1007/s41024-022-00208-8

RESEARCH ARTICLE

Achieving energy efficiency and thermal comfort through passive strategies and renewable technology. Wuhai demonstration center project as an application case

Stahel Serano Bibang Bi Obam Assoumou[1] · Zhu Li[1]

Received: 5 March 2022 / Revised: 12 June 2022 / Accepted: 14 June 2022 / Published online: 6 August 2022

Abstract
Buildings are designed to meet and improve the quality of life of the occupants. During the last decades, standards on building construction have risen sharply to integrate new, ambitious demands regarding energy efficiency and thermal comfort in the design procedure. The importance of understanding the performance of a proposed building project is undeniable nowadays. This paper presents a building performance assessment of the proposed demonstration center in Wuhai. The analysis of this paper focus on thermal comfort and energy performance through the application of passive solutions and renewable technology. The purpose of this study is to predict energy efficiency and thermal comfort through an effective simulation assessment of a proposed project at the design stage. Using parametric study, it is concluded that in this well-designed project, when appropriate building parameters are used, very little amount of energy is required for heating and cooling to maintain a comfortable indoor temperature. Also, the total amount of energy generated through solar PV remains higher than the total energy consumption, which makes the building energy self-sufficient. Additionally, the same parameters result in a high level of thermal comfort, which improve the occupants' comfort and well-being. The findings indicate that incorporating appropriate passive strategies and renewable technology during the design stage has a beneficial effect on the entire building performance. Some good practices have also been highlighted and documented in this study.

Keywords Energy efficiency · Thermal comfort · Passive strategies · Renewable technology · Simulation · Demonstration center

1 Introduction

Concerns about buildings' environmental effect and the quality of their indoor environment have sparked debate over the role the design team should play in environmental design [1]. Passive design, often known as "bio-climatic design," seeks to improve residents' comfort and health by incorporating local climatic and site elements into architectural design and building technologies [2]. As defined by Olgyay in their early studies, the purpose of passive design is to heat, cool, and light buildings using new adaptive ideas and materials while reducing or even eliminating the use of any energy system [3]. Local builders have successfully adopted numerous passive design strategies, such as a north–south plan orientation to balance solar gains, window openings designed to promote natural ventilation from local winds, external overhangs to protect from direct sunlight in the summer, and courtyards to offer a filtering area with the surrounding environment [4, 5].

It is becoming increasingly recognized that, in the end, the performance of a building is largely determined by its "strategic" design as considered during the project's early stages. For example, plan depth, orientation, fenestration (glazing) and natural ventilation, affect the amount of heating and cooling required. These early design decisions invariably have knock-on effects on plants and equipment, which have a significant impact on the entire building performance [6]. In recent years, much effort has been put into the development of efficient and cost-effective technologies, to ensure the sustainability of the built environment [7, 8]. However, in addition, to reduce energy demand while having

✉ Stahel Serano Bibang Bi Obam Assoumou
bibangserano@gmail.com; bibang@tju.edu.cn

Zhu Li
zhuli1977@tju.edu.cn

[1] School of Architecture, Tianjin University, Tianjin, China

sustainability concerns, buildings must also provide comfort for their occupants [9]. This may create a conflict between strategies that focus on the reduction of energy consumption and those to maintain a healthy and comfortable indoor environment. To achieve a balance between efficiency and comfort, synergies between building design, have to be established [10]. The present study set out for a parametric building performance simulation on the impact of passive strategies and renewable technology under the Wuhai climatic condition to predict energy efficiency and thermal comfort of a proposed project at the design stage.

2 Methods

The method of this paper is divided into two sections. The first section describes the project, including climate conditions, passive design implementation, and renewable energy application. The second section presents the simulation process with parametric concept analysis. The last section deals with energy performance and thermal comfort analysis.

2.1 Project description

2.1.1 The climatic condition of Wuhai

According to the Köppen climate classification, the climate on the Wuhai is a cold arid desert climate. This climate is characterized by freezing, dry winter, and hot summers [11]. The cold desert climate is also found in several regions outside western china such as Morocco, South Africa, and Turkestan. To be more specific, according to the Köppen climate classification, Wuhai climate is a cold arid desert climate (BWk) [12]. The map in Fig. 1 shows the regions that feature such a climate.

Table 1 presents the information on the Wuhai weather and denotes the period for the acquisition of original weather data. All-weather data used in the present study were taken

Table 1 Information on the Wuhai weather as well as on the period the data acquisition (data source: weatherbase.com)

Wuhai, China	
Latitude	39.6538° N
Longitude	106.7955° E
Altitude	1096 m a.s.l
Time period for data acquisition	2020–2022

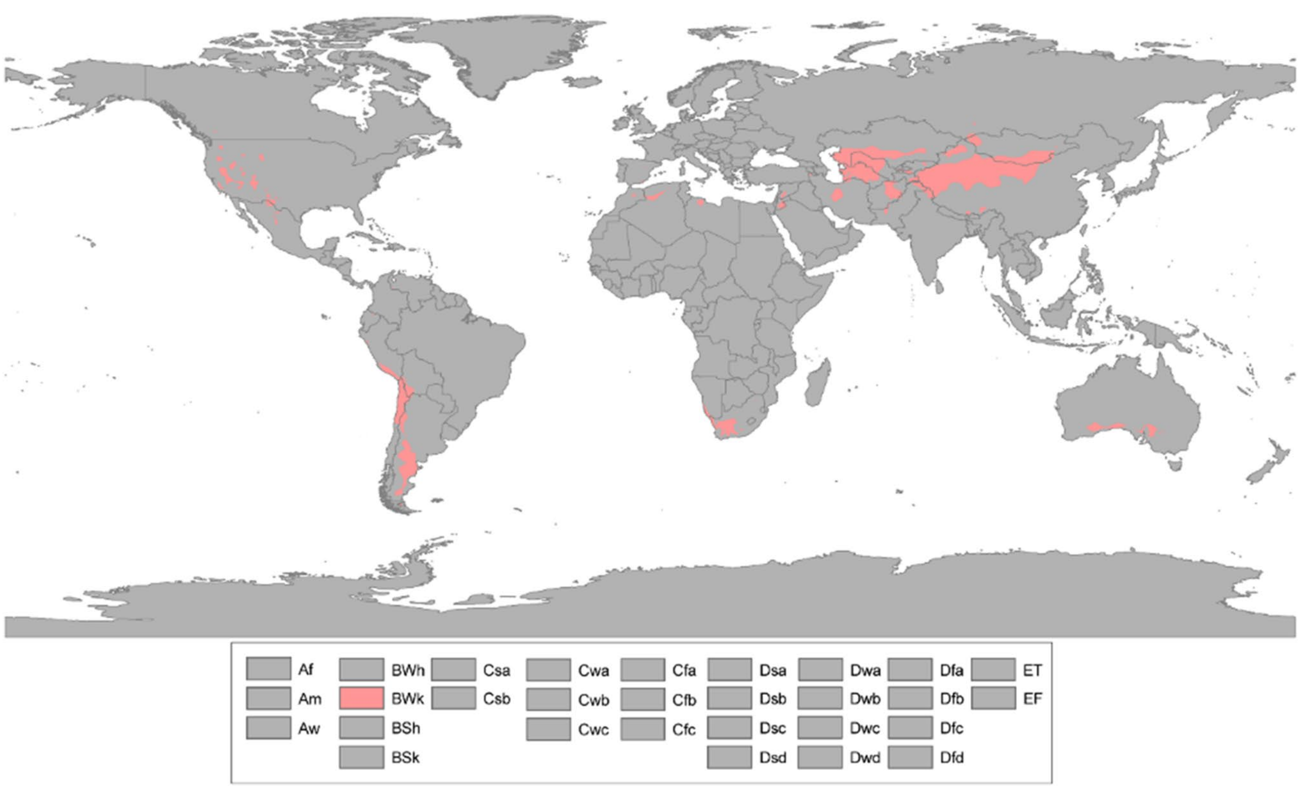

Fig. 1 Regions with a cold arid desert climate (BWk) according to the world map Köppen climate classification [12]

Table 2 Monthly and annual mean values of weather data for Wuhai, China (data source: weatherbase.com)

Month	Average high temperature (℃)	Average humidity (−)	The average length of the day (hours)	Wind speed (m/s)
Jan	−3.8	16.1	10.2	6.5
Fev	0.2	14.1	11.2	7.9
Mar	7.7	8.2	12.4	9.7
Apr	16.1	2.4	12.4	11.5
May	23.0	4.6	14.9	10.8
Jun	27.4	10.7	15.5	9.4
Jul	29.0	15.5	15.2	8.3
Aug	27.0	14.8	14.2	7.2
Sep	21.6	9	12.9	6.8
Oct	14.6	1.7	11.6	6.8
Nov	5.0	6.3	10.5	7.2
Dec	−2.2	13.3	9.9	6.5
Year	13.8	0.1	12.7	8.2

from a meteorological database called weather base (www.weatherbase.com). Table 2 shows the monthly mean values of average high temperature, average relative humidity, the average length of the day, and wind speed.

2.1.2 Project setting

The project is located in Wulannur Town, Wuda District, under the administration of Wuhai City, 18 km away from the downtown of Wuhai City, 13 km away from Wuda District, and 43 km away from Hainan District (Fig. 2), under the climate condition shown in Table 2. With renewable energy as the core, the Wuhai demonstration center design has combined the top teams in various fields such as planning, design, construction, planting, operation, management, and more, from both domestic and foreign expertise to form a cross-border consortium to come up with an appropriate design which could be replicable anywhere depending on the climate conditions.

The Demonstration center accommodates various functional spaces which come together to create a harmonious

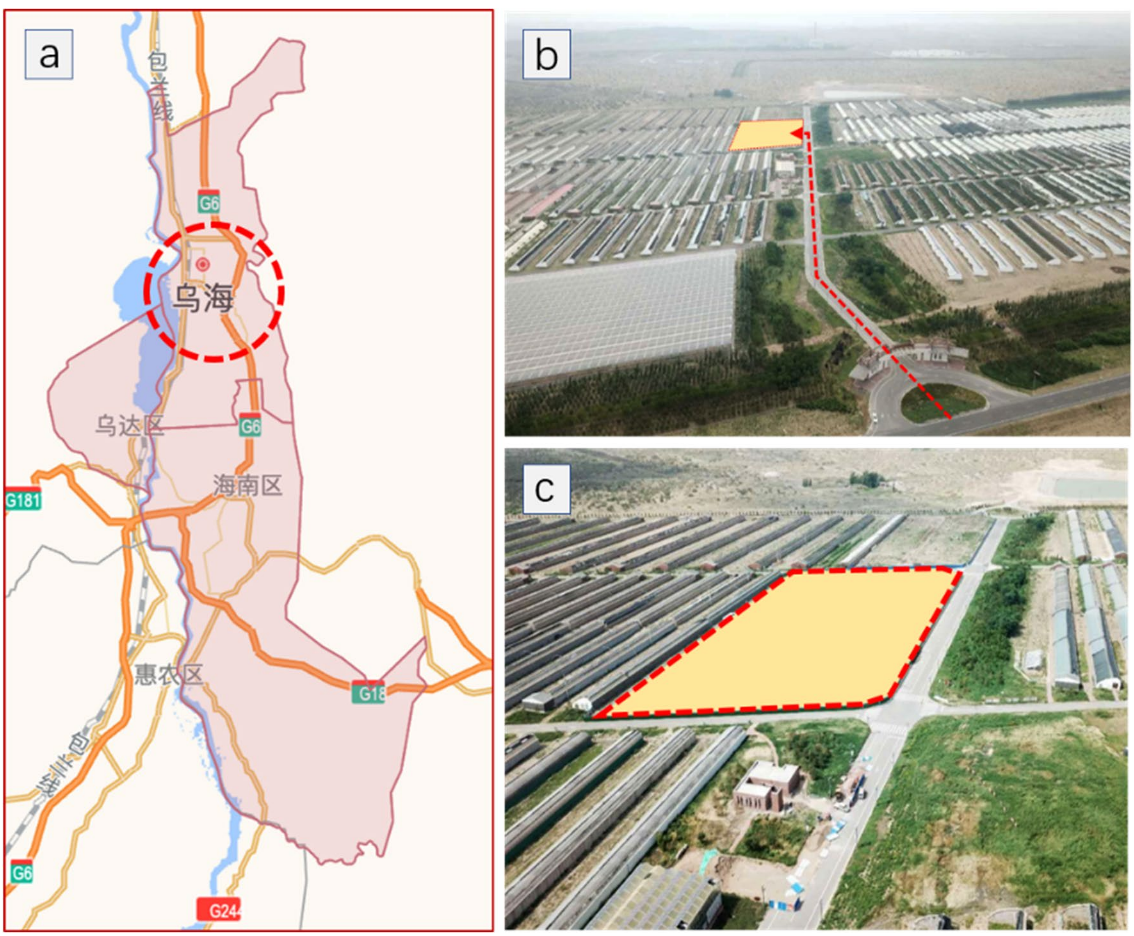

Fig. 2 Site location of Wuhai city, **a** Google map showing the entire territory with Wuhai as the center. **b** Aerial view of the project site and accesses from the main road. **c** A close aerial view of the site for the agricultural demonstration park

environment. The design was done in such a way that it could address healthy environmental issues by improving the quality of life of the occupants when completed. The Demonstration Center is designed on three floors and includes the following areas; colonnade space, exhibition area, exchange area, experience dining room, conference rooms, office area, accommodation area, and indoor garden. Table 3 below presents the project program and Fig. 3 shows subsequent floor plans.

2.1.3 Passive design strategies

The cornerstone of passive design is based on natural energy sources, which combines building architecture and the surrounding environment to reduce heating and cooling loads of structures while minimizing operating and maintenance costs [13, 14]. One of the key aspects of the passive design approach to reducing energy use and increasing occupant thermal comfort is the correlation of local climate with building shape and thermal performance [15]. The passive strategies used at the Wuhai demonstration center rely on the local climate to maintain the thermal range of buildings within spaces, avoiding the need for mechanical heating, ventilation, and cooling. The key strategy was to design with the local climate in mind. For best production, the design team needed to blend passive techniques with the surrounding local climate.

Figure 4 presents the sun shading chart for winter and summer that was examined by the design team in order to fully utilize passive solar design features and maximize the energy efficiency, comfort.

The following sections present the various passive strategies and renewable energy technology adopted during the design stage of the Wuhai demonstration center.

Table 3 Demonstration center program

Demonstration center		
Floors	Spaces	Areas
Floor 1	Colonnade space	200 m^2
	Reception	105 m^2
	Exhibition area	460 m^2
	Exchange area	250 m^2
	Multi-purpose area	305 m^2
	Eating area	305 m^2
	Offices	125 m^2
Floor 2	Conference area	220 m^2
	Offices	286 m^2
	Open office	181 m^2
	Meeting room	161 m^2
Floor 3	Leading office area	161 m^2
	Accommodation area	428 m^2
	Terrace garden	405 m^2
Total open area		633 m^2
Total service area		544 m^2
Total floor area		4769 m^2

2.1.3.1 Building orientation and shape When designing, the orientation of the site as well as the building shape was taken into consideration, this influences the building design as it helps to maximize the effectiveness of other passive strategies. The design of the Wuhai demonstration center uses simple rectangular shape with longitudinal orientation, along the sun path to guarantee an efficient passive design as shown in Fig. 5. The rectangular shape allows (1) the roof to be the main heat gain element of the structure, (2) the south facade to collect sun all year round, (3) the north façade to enhance natural ventilation with multiple opening, and (4) The west and east façades to be the second most exposed element in the building with small openings.

2.1.3.2 Shading potential To maximize energy savings, shading devices should be included into the facade of a structure from the early design stage. This can be accomplished through the use of "conventional" design tools such as solar path diagrams and shading masks, or through the use of specialized computer algorithms that "generate" the optimal shading device shape based on a set of input parameters [16]**.** This information allows the design team to make meaningful hypotheses about the optimum geometry of the shading device. According to the solar shading chart in Fig. 6, horizontal shading devices installed at the Wuhai agricultural demonstration park during the winter should be set at 75° This is to maximize winter sun collecting in the south while shielding users from visual intrusion. The shading devices are set to 60° during the summer to provide a maximum of four hours of shade. Additional vertical strips are utilized to enhance indoor thermal comfort and provide enough shading.

2.1.3.3 Natural ventilation and daylight Passive ventilation strategies in this project use naturally occurring airflow patterns around and in the building to introduce outdoor air into the space. The Demonstration center takes advantage of this feature through it north–south orientation and the operable windows, especially during the summertime. Additionally, to enhance the quality of light and assure appropriate distribution within spaces, a high window to wall area ratio at the south façade paired with high ceilings is provided. Extra features such as interior surface colors and finishes are also considered. Figure 7 shows the light admission during summer and winter.

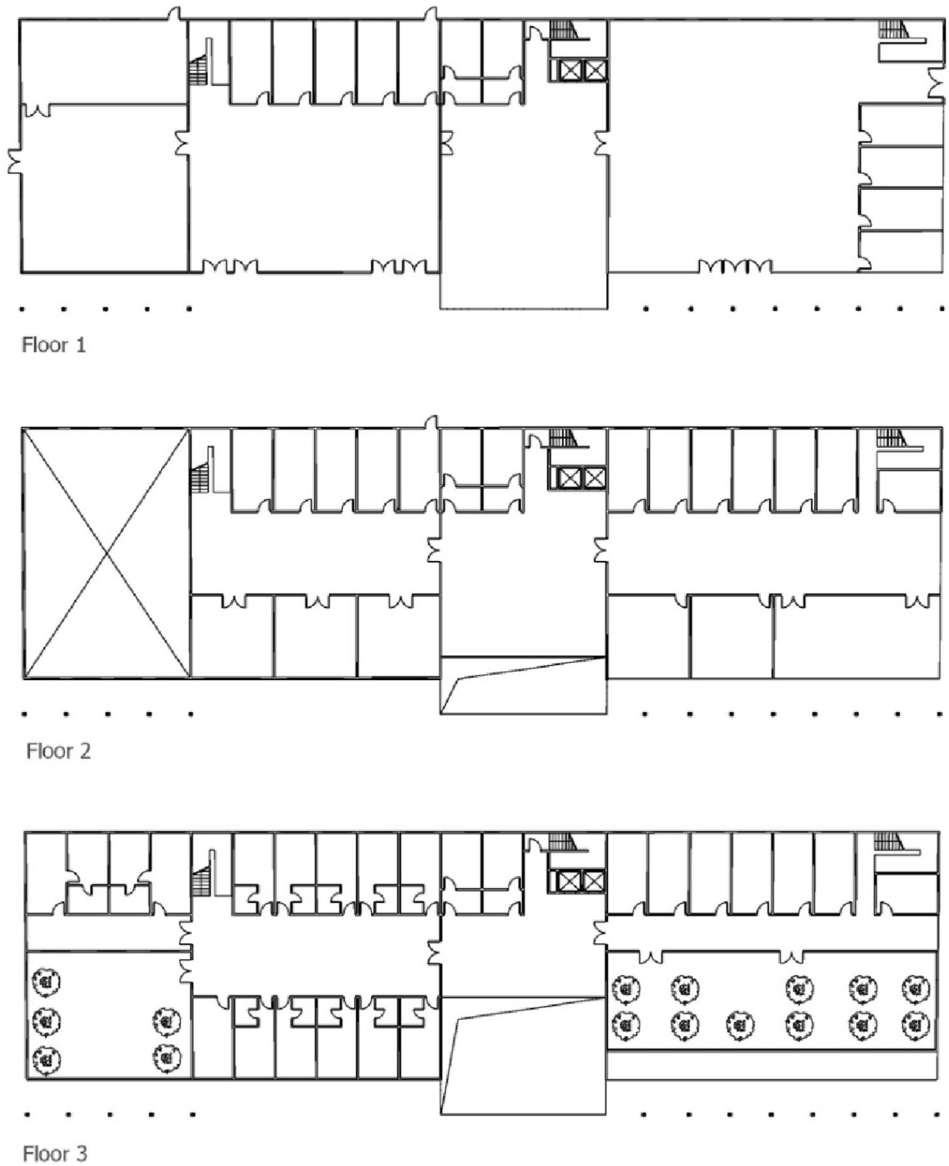

Fig. 3 Demonstration center floor plans

2.1.3.4 Building envelope The analysis from the Psychometric chart helps to easily engage in the process of passive heating and cooling, elements of the building envelop were set as follow: high-performance and operable windows with low wall area ratio on the north façade for winter sun exposure, High-performance window with high wall area ratio on the south façade for solar heat gain (Fig. 8). Appropriate shading devices were provided to shade the building on the south during summer. The wall and the floor slab are high thermal mass surfaces that store winter passive heat and summer night cool. The floor plans are designed to allow winter sun penetration into offices and outdoor spaces are protected with a large overhang with integrated roof shading.

2.1.4 Renewable energies technologies

Because the project is located in a remote area, away from the main city grid. One of the simplest ways to be connected with constant energy is through renewable energy technologies which produce sustainable and clean energy from sources. Renewable energy has the potential to strengthen energy security, improve environmental quality and contribute to the widespread diffusion of energy availability [17]. For this project, the focus is on solar PV with a system that will ensure the transformation of solar radiation into electricity. To implement this system, the design team proceeded with an analysis of the solar path in view to provide solar panels where needed and make appropriate use of the sun

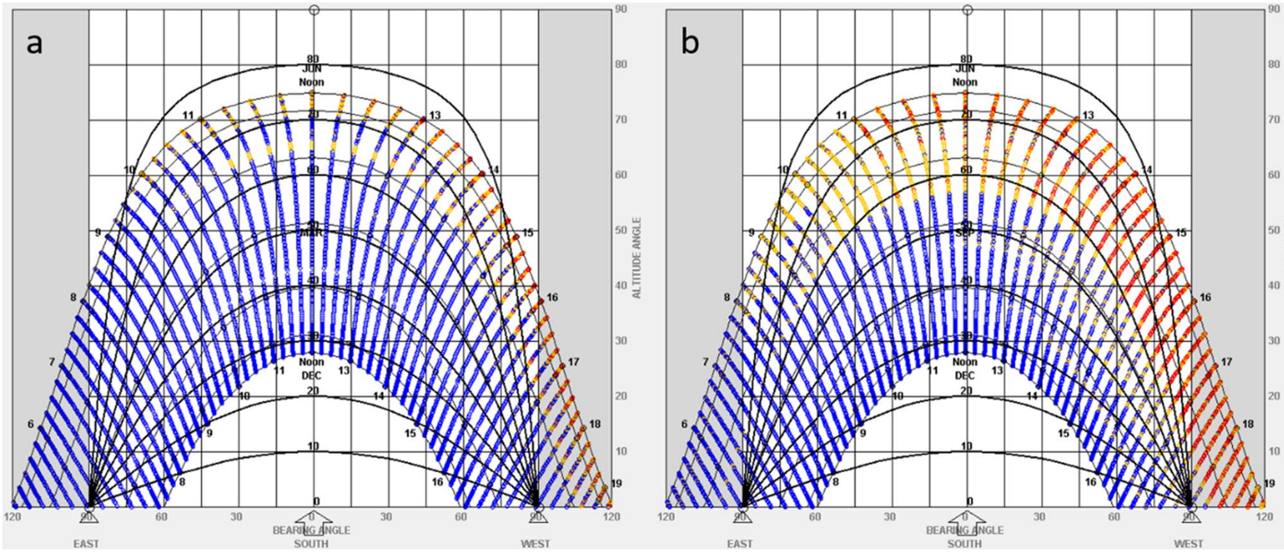

Fig. 4 **a** Sun shading chart during winter **b** sun-shading chart during summer

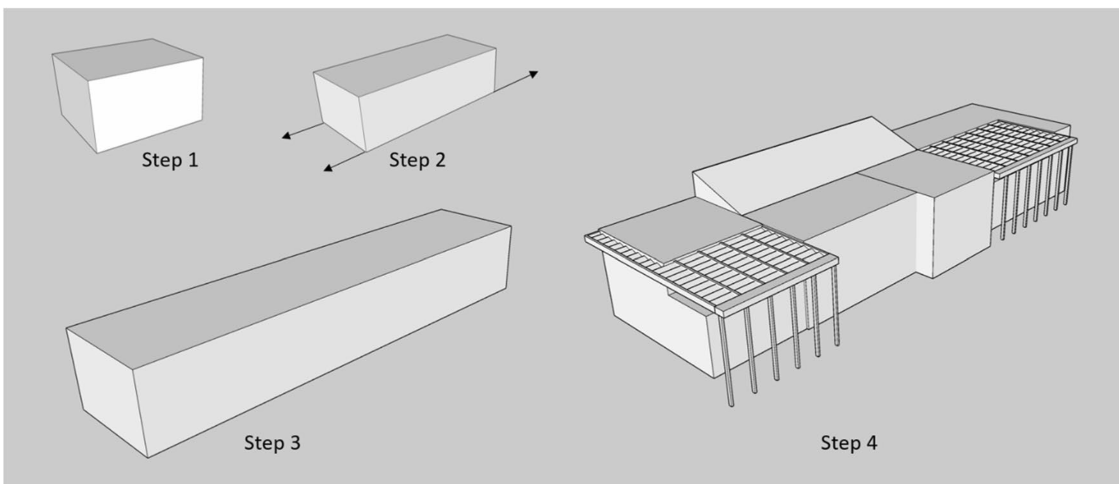

Fig. 5 Shape development in response to sun path and wind direction

as natural and renewable energy. Figure 9 shows the sun's path as it affects the length of daytime experienced and the amount of daylight received along a certain latitude during the summer and the winter solstice.

2.1.4.1 Solar panel system Architectural integration represents an interesting opportunity for photovoltaic since the installation of modules on the building envelope provides a variety of advantages, such as the use of the land surface already occupied by the building, the saving on support structures, the replacement of materials and components such as traditional roof elements and the possibility of the energy produced on-site. However, to obtain the best performance, careful planning is necessary. The placement and orientation of solar panels are just as important as which type of solar panel is used in a given situation. A solar panel will harness the most power when the Sun's rays hit its surface perpendicularly [18, 19]. Ensuring that solar panels face the correct direction and have an appropriate tilt will help ensure that they produce maximum energy as they are exposed to the highest intensity of sunlight for the greatest period [20]. Figure 10 shows solar PV location on the demonstration center.

In the northern hemisphere, solar panels should face the south. Usually, this is the best direction because solar panels will receive direct light throughout the day [20]. The angle or tilt of a solar panel is also an important consideration. The angle that a solar panel should be set at to produce the most

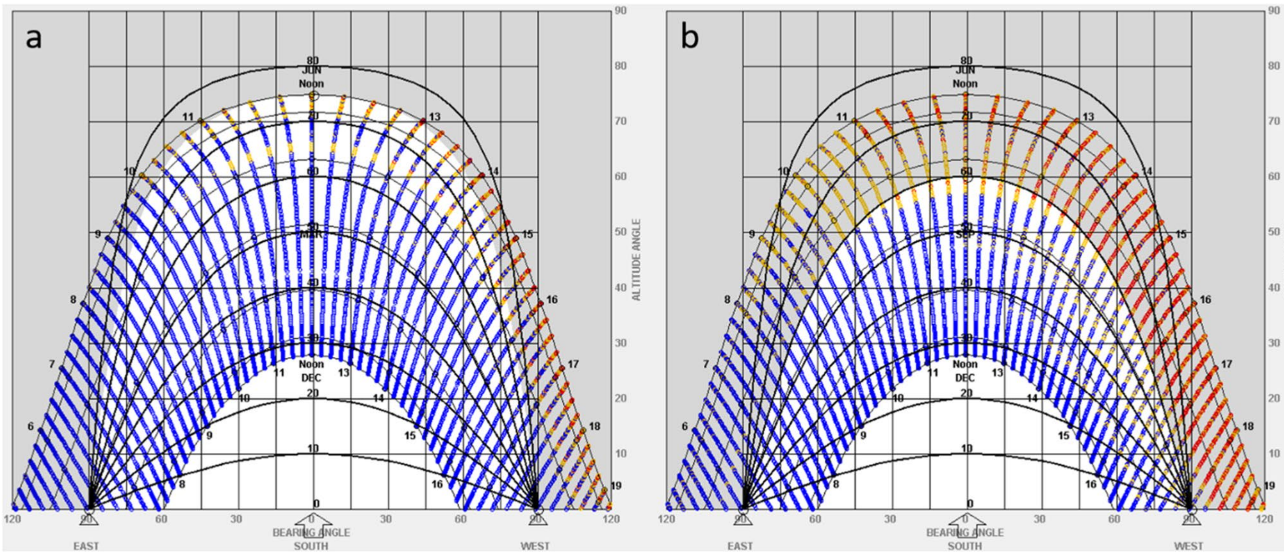

Fig. 6 **a** Sun shading chart used to design vertical and horizontal shading devices during winter **b** sun-shading chart used to design vertical and horizontal shading devices during summer

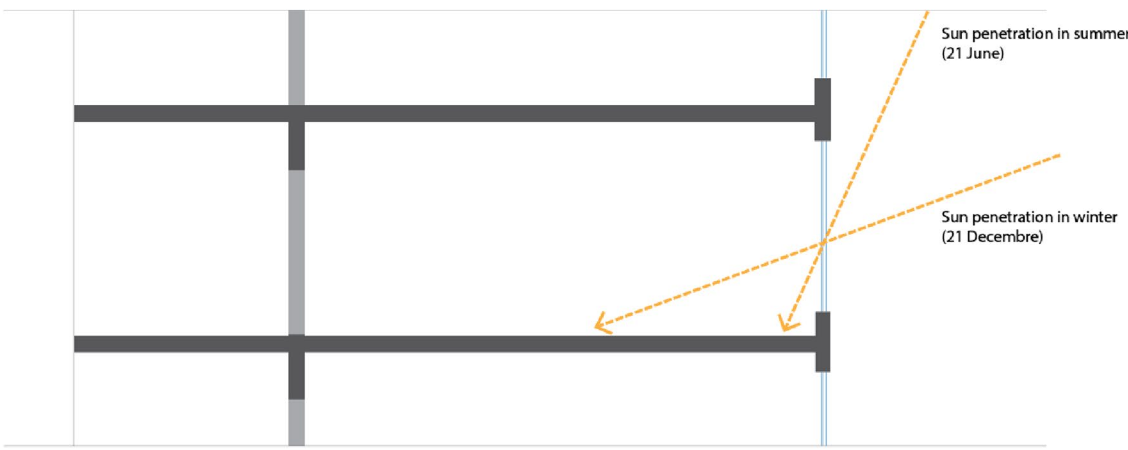

Fig. 7 Light admission during summer and winter

energy in a given year is determined by the geographical latitude. A general rule for optimal annual energy production is to set the solar panel tilt angle equal to the geographical latitude [21]. The Wuhai is located at the latitude 39.65°. Therefore the solar panels were all fixed at 39°. Figure 11 presents displacements of solar PV on different sections of the building.

2.2 Building performance simulation

2.2.1 Simulation method

A 3D conceptual model was first created in SketchUp, then the model was imported to Revit where walls, roofs, floors, door and windows assembly were properly adjusted. Next, the developed Revit model was exported in gbXML format for energy simulation in DesignBuilder software. The plan of the building was divided into various separate HVAC zones including Reception, Exhibition area, Multi-purpose area, Cooking and eating area, Conference room, offices, meeting room and accommodation area. The cooling temperature was set at 24 ℃, while the heating was set at 22 ℃. Simulations for the energy model were conducted in Wuhai, New Mongolia, china and the weather data provided by EnergyPlus for the location were used. Physical properties and parameters were defined as described in Table 4. Other model information settings for each space including material, occupancy schedule, Window and door

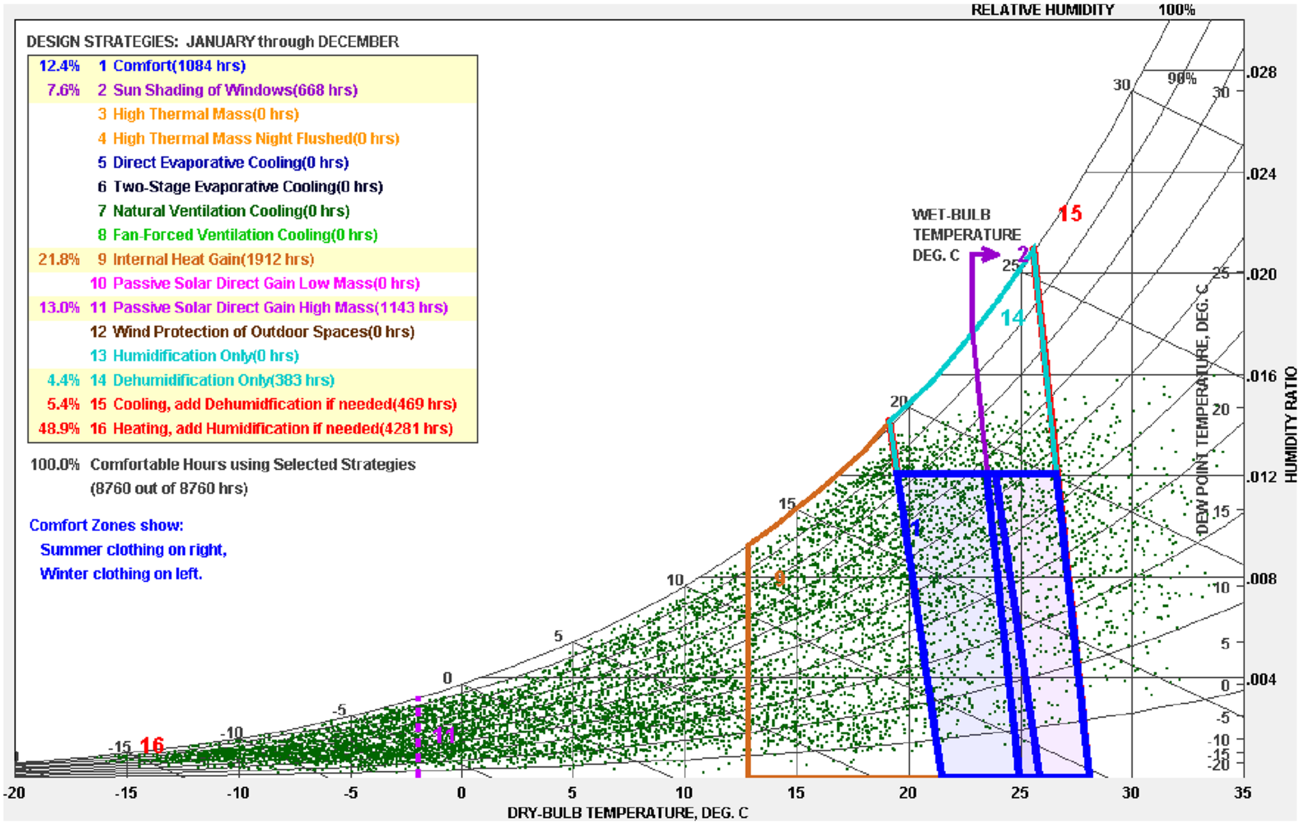

Fig. 8 Psychometric chart to evaluate thermal comfort through appropriate design strategies

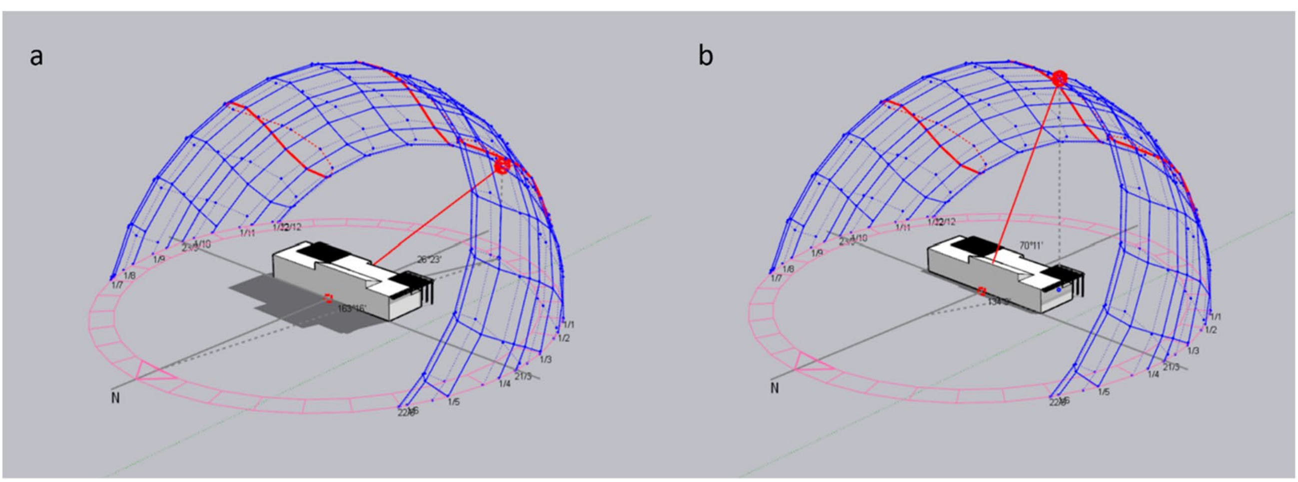

Fig. 9 **a** Sun shade direction on the winter solstice, and **b** the winter solstice

materials, lighting power were adopted. Activity parameter was set according to ASHRAE 55. Once everything was set in place, we ran the simulation process for the demonstration center.

2.2.2 Reference case-building model

A base case building model of the demonstration center was set up in DesignBuilder based on the assumption of a fully detached, cuboid-shaped, building, where all façades were fully exposed to solar radiation and each floor had a

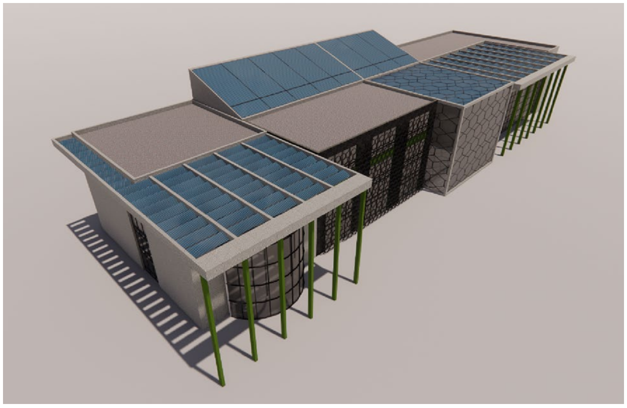

Fig. 10 Top aerial view from the south-west showing a full display of the demonstration park covered with solar panels (in blue)

gross floor area of 1725 m^2. Assuming different geometry, construction and use for each floor, the full building has to be modeled. The whole building was modeled as a single zone having, therefore, only one operative room temperature. Table 4 shows the parameters of walls, roof as well as window (glazing) assemblies. Figure 12 displays the DesignBubilder model. Architecturally, the thermal transmittances of the external walls and the glazing were specified as 2.223 W/m^2 k and 7.121 W/m^2 k, respectively. The total solar energy transmittance (g) of all windows was defined as 0.81.

In the present study, the adaptive model of the ASHRAE 55 [22] was employed for assessing the thermal comfort of the demonstration center, which refers to buildings without mechanical means systems and with operable windows. In this empirically derived adaptive thermal comfort concept, the range of acceptable operative room temperatures is defined as a function of the running mean of the interior temperature. Based on ASHRAE standard 55 using PMV, the highest acceptable comfort temperature is 24.3 ℃ during winter and 26.7 ℃ during summer, while the lowest acceptable comfort is 20.3 ℃ for both periods [22]. Only office hours were used in this analysis. The operative room temperature is calculated in DesignBuilder as the mean value of the air temperature and the mean radiant temperature in the room. The latter is defined as the area-weighted mean surface temperature of the enclosures (walls, roof, and

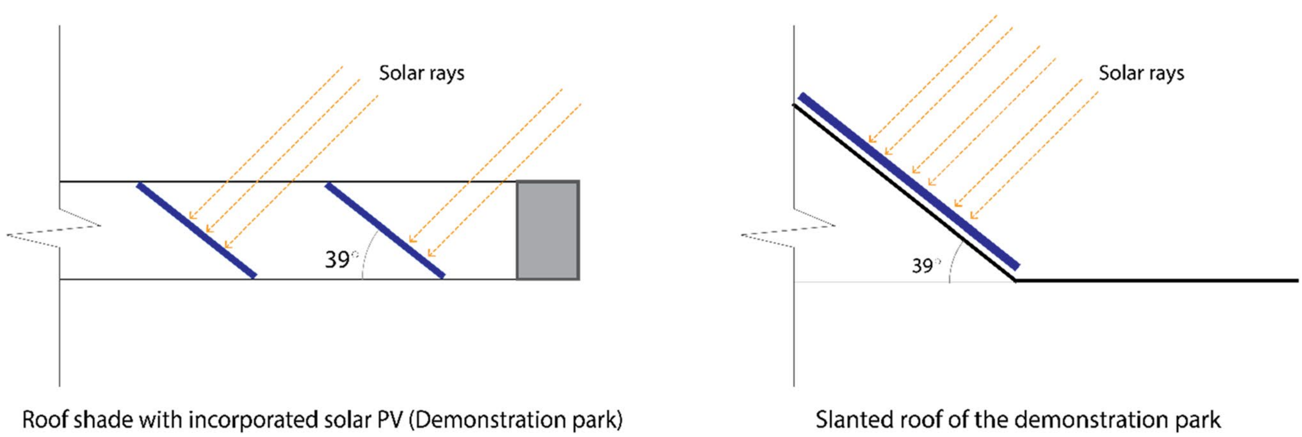

Fig. 11 Sectional views of solar PV on demonstration park and smart greenhouse

Table 4 Parameters of walls, roof as well as window (glazing) assemblies

Case 1—base case								
Glazing Sgl Clr 6 mm			Concrete roof (BS EN ISO 6946)			Brick wall (BS EN ISO 6946)		
Specification	Value	Unit	Specification	Value	Unit	Specification	Value	Unit
Total solar transmission	0.81	SHGH	Thickness	0.2	m	Thickness	0.2	m
Direct solar transmission	0.775		Upper resistance limit	0.317	m^2 k/W	Upper resistance limit	0.448	m^2 k/W
Light transmission	0.881		Lower resistance limit	1.317	m^2 k/W	Lower resistance limit	0.448	m2 k/W
U-value (ISO 10292/EN 673)	6.121	W/m^2 k	U-value surface to surface	5.65	W/m^2 k	U-value surface to surface	3.6	W/m^2 k
U-value	7.121	W/m^2 k	R-value	0.317	m^2 k/W	R-value	0.448	m^2 k/W
			U-value	3.155	W/m^2 k	U-value	2.233	W/m^2 k

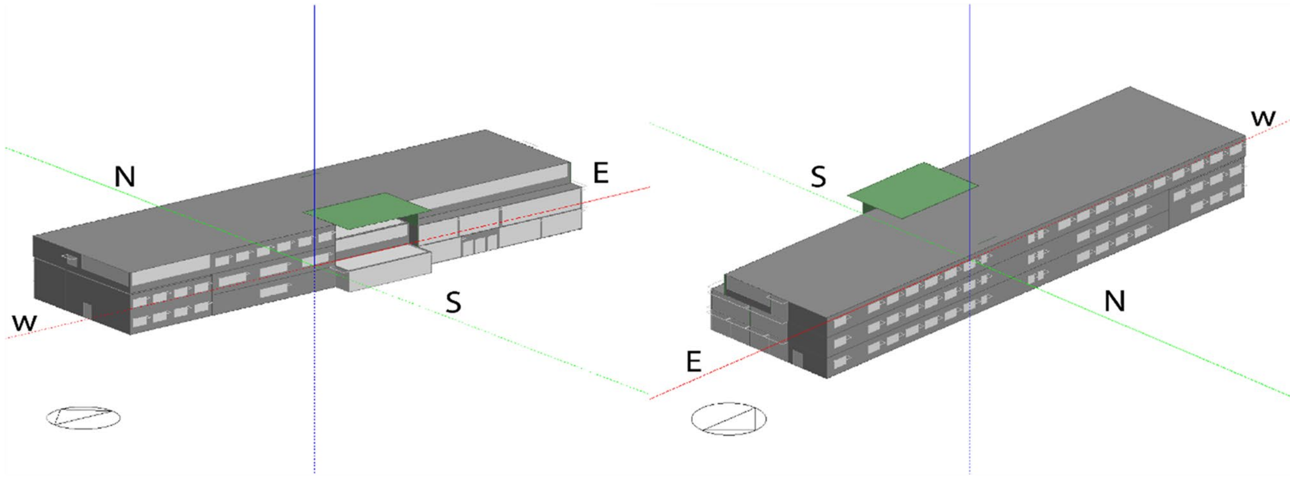

Fig. 12 Reference case (Designbuilder) model of the demonstration center

windows). The influence of other room parameters such as the relative humidity on the adaptive thermal comfort was not included in the model.

2.2.3 Parametric study

To better understand the impact of input variables on energy consumption and thermal comfort and test the robustness of results, a parametric study was performed. The present study also shows how sensitive the results are to a change of certain input variables. Starting from the reference case described in Sect. 5.8, a series of case scenarios methods were used to show the effect of the variation of the wall assembly, roof assembly, and window assembly on the level of energy-saving and thermal comfort that can be achieved. Input parameters were varied according to scenarios presented from table 5 to table 8. In scenario case 2, the external wall thickness was set to 0.2770 m, with a resistance limit of 1.302 m^2 k/W and a transmittance value of 0.768 W/m^2 k (Table 5). In scenario case 3, the concrete roof was set at a resistance limit of 1.949 m^2 k/W and a transmittance value of 0.513 W/m^2 k (Table 6). In scenario case 4, the window assembly was set to triple glazing (Tpl LoE (33) Bronze 6 mm/13 mm Air), with a total solar transmission (g) of 0.142 and a transmittance value of 1.999 W/m^2 k (Table 7). The last scenario case 5 is the one that combines scenarios cases 2, 3, and 4, where the wall, the roof and window assembly were all replaced (Table 8).

2.3 Energy performance and thermal comfort analysis

2.3.1 Energy performance

The energy performance of a building depends on the quality of the properties of the building itself, it is a critical factor that determines how much energy the building consumes. Building performance relies on passive and active strategies applied during the design process. Table 8 (Case 5) outlined the optimized case scenario with an optimized building envelope of the Demonstration center building.

Table 5 Scenario case—2, wall assembly was replaced

Case 2—efficient wall								
Glazing Sgl Clr 6 mm			Concrete roof (BS EN ISO 6946)			Brick wall (BS EN ISO 6946)		
Specification	Value	Unit	Specification	Value	Unit	Specification	Value	Unit
Total solar transmission	0.81	SHGH	Thickness	0.2	m	Thickness	0.277	m
Direct solar transmission	0.775		Upper resistance limit	0.317	m^2 k/W	Upper resistance limit	1.302	m^2 k/W
Light transmission	0.881		Lower resistance limit	1.317	m^2 k/W	Lower resistance limit	1.302	m^2 k/W
U-value (ISO 10292/EN 673)	6.121	W/m^2 k	U-value surface to surface	5.65	W/m^2 k	U-value surface to surface	0.883	W/m^2 k
U-value	7.121	W/m^2 k	R-value	0.317	m^2 k/W	R-value	1.302	m^2 k/W
			U-value	3.155	W/m^2 k	U-value	0.768	W/m^2 k

Table 6 Scenario case—3, roof assembly was replaced

Case 3—efficient roof								
Glazing Sgl Clr 6 mm			Concrete roof (BS EN ISO 6946)			Brick wall (BS EN ISO 6946)		
Specification	Value	Unit	Specification	Value	Unit	Specification	Value	Unit
Total solar transmission	0.81	SHGH	Thickness	0.132	m	Thickness	0.2	m
Direct solar transmission	0.775		Upper resistance limit	1.949	m^2 k/W	Upper resistance limit	0.448	m^2 k/W
Light transmission	0.881		Lower resistance limit	1.949	m^2 k/W	Lower resistance limit	0.448	m^2 k/W
U-value (ISO 10292/EN 673)	6.121	W/m^2 k	U-value surface to surface	0.553	W/m^2 k	U-value surface to surface	3.6	W/m^2 k
U-value	7.121	W/m^2 k	R-value	1.949	m^2 k/W	R-value	0.448	m^2 k/W
			U-value	0.513	W/m^2 k	U-value	2.233	W/m^2 k

Table 7 Scenario case—4, *w*indows (*g*lazing) assembly was replaced

Case 3—efficient glazing								
Efficient glazing Trp LoE Film 6 mm/13 mm Air			Concrete roof (BS EN ISO 6946)			Brick wall (BS EN ISO 6946)		
Specification	Value	Unit	Specification	Value	Unit	Specification	Value	Unit
Total solar transmission	0.142	SHGH	Thickness	0.2	m	Thickness	0.2	m
Direct solar transmission	0.073		Upper resistance limit	0.317	m^2 k/W	Upper resistance limit	0.448	m^2 k/W
Light transmission	0.169		Lower resistance limit	1.317	m^2 k/W	Lower resistance limit	0.448	m^2 k/W
U-value (ISO 10292/EN 673)	1.99	W/m^2 k	U-value surface to surface	5.65	W/m^2 k	U-value surface to surface	3.6	W/m^2 k
U-value	1.99	W/m^2 k	R-value	0.317	m^2 k/W	R-value	0.448	m^2 k/W
			U-value	3.155	W/m^2 k	U-value	2.233	W/m^2 k

Table 8 Scenario case—5, wall, roof and windows assembly were replaced

Case 5—efficient wall/roof/glazing								
Efficient glazing Trp LoE film 6 mm/13 mm Air			Concrete roof (BS EN ISO 6946)			Brick wall (BS EN ISO 6946)		
Specification	Value	Unit	Specification	Value	Unit	Specification	Value	Unit
Total solar transmission	0.142	SHGH	Thickness	0.132	m	Thickness	0.277	m
Direct solar transmission	0.073		Upper resistance limit	1.949	m^2 k/W	Upper resistance limit	1.302	m^2 k/W
Light transmission	0.169		Lower resistance limit	1.949	m^2 k/W	Lower resistance limit	1.302	m2 k/W
U-value (ISO 10292/EN 673)	1.99	W/m^2 k	U-value surface to surface	0.553	W/m^2 k	U-value surface to surface	0.883	W/m^2 k
U-value	1.99	W/m^2 k	R-value	1.949	m^2 k/W	R-value	1.302	m^2 k/W
			U-value	0.513	W/m^2 k	U-value	0.768	W/m^2 k

2.3.1.1 Energy production from solar panel In terms of energy, the Wuhai agricultural demonstration park is designed to provide maximum energy to sustain its annual consumption. To help achieve this result, the buildings were all designed to facilitate the positioning of PV panels on their roofs which have a triangulated form and mostly face the south. Additional PV pods were provided on site to maximize energy collection. Table 9 presents the zoning with their respective spaces as well as the total PV collection surface and their yearly energy generation.

2.3.1.2 Energy consumption The focus of this analysis remains the demonstration center which is the main building of this project. It is a mixed-use building where various activities take place including, working, living, eating and recreational. Figure 13, Fig. 14, Fig. 15, Fig. 16 and Fig. 17 show the monthly energy consumption in electricity for lighting, heating and cooling of case 1, case 2, case 3, case 4, and case 5.

Table 9 Total energy generation from the entire agricultural demonstration park

Zoning	Spaces	PV Area (m^2)	Annual AC Energy (kWh)
Building complex	Product supply center	317	70,483
	Demonstration center	963	214,414
Smart greenhouse	Smart greenhouse	1993	508,167
	PV pods	65	16,489
Energy plaza	Energy tree	264	58,761
	Energy tree outdoor area	92	20,476
	Plaza	51	11,426
	Plaza PV pods	5	1,186
	Reception	46	10,090
	Parking area	307	68,257
	Entrance PV pods	19	4,155

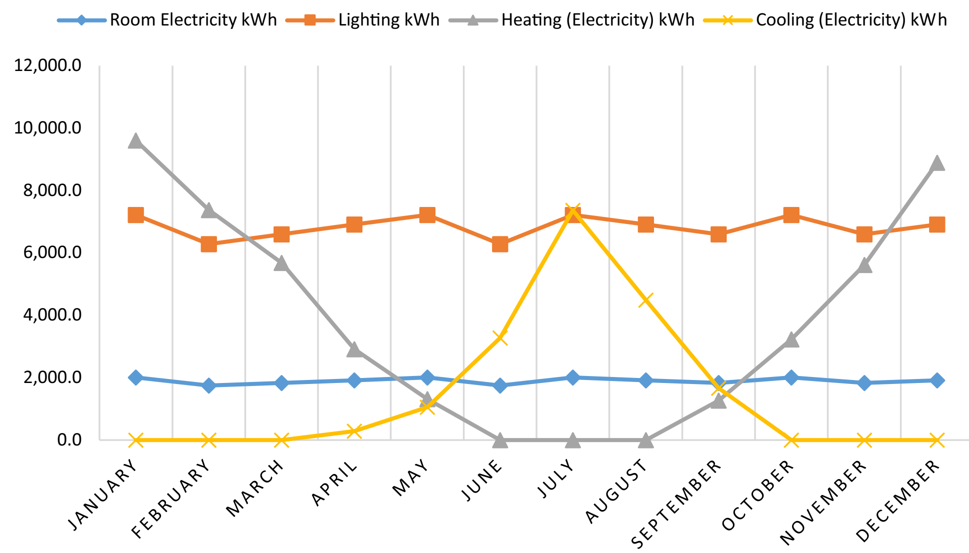

Fig. 13 Monthly energy consumption from case 1—base case

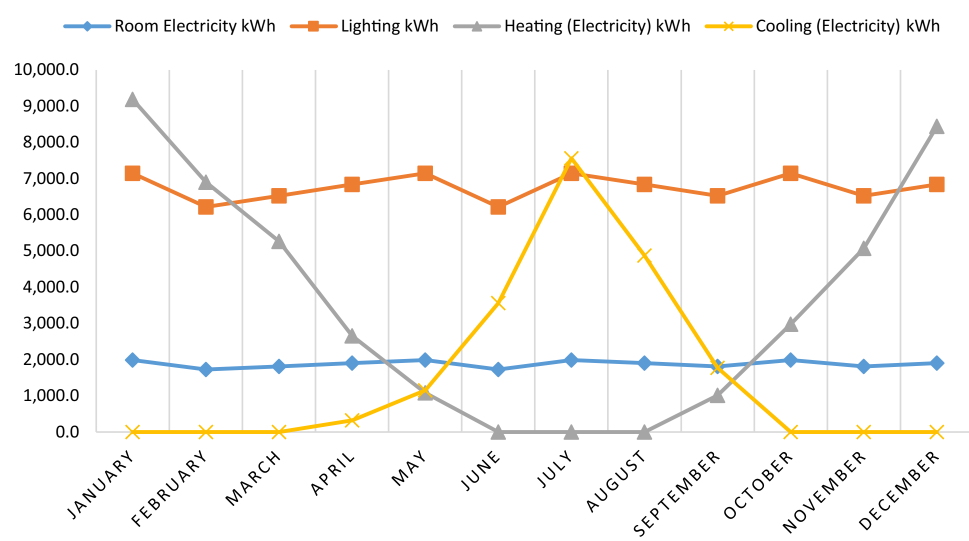

Fig. 14 Monthly energy consumption from case 2—efficient wall

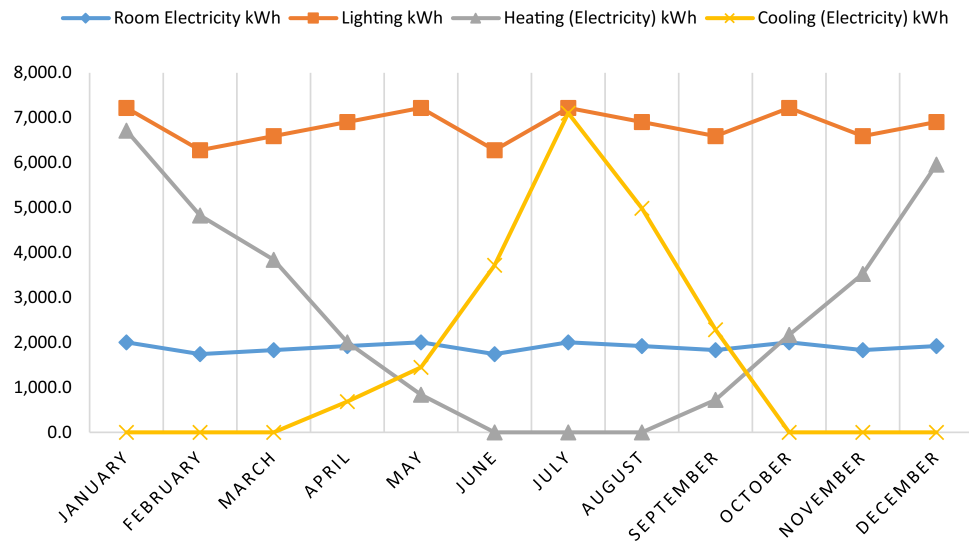

Fig. 15 Monthly energy consumption from case 3—efficient roof

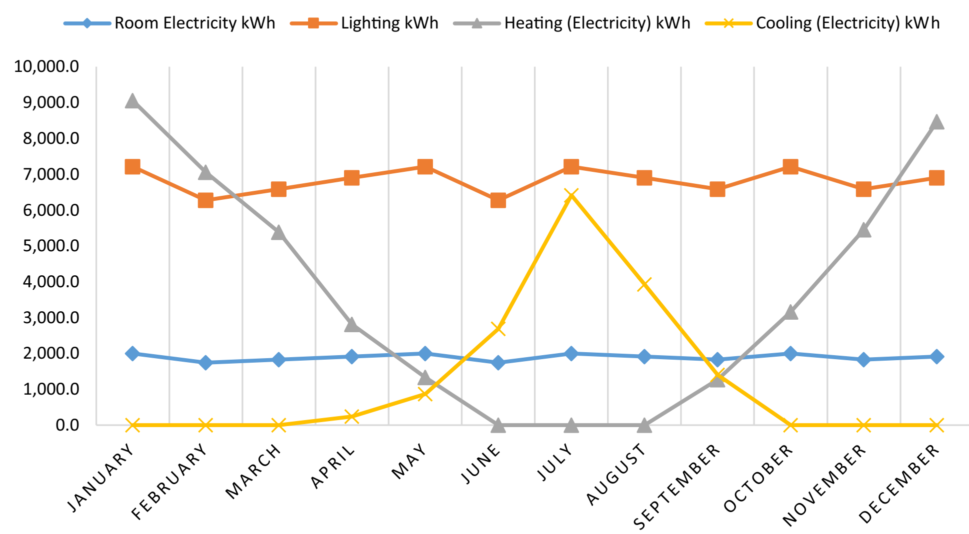

Fig. 16 Monthly energy consumption from case 4—efficient glazing

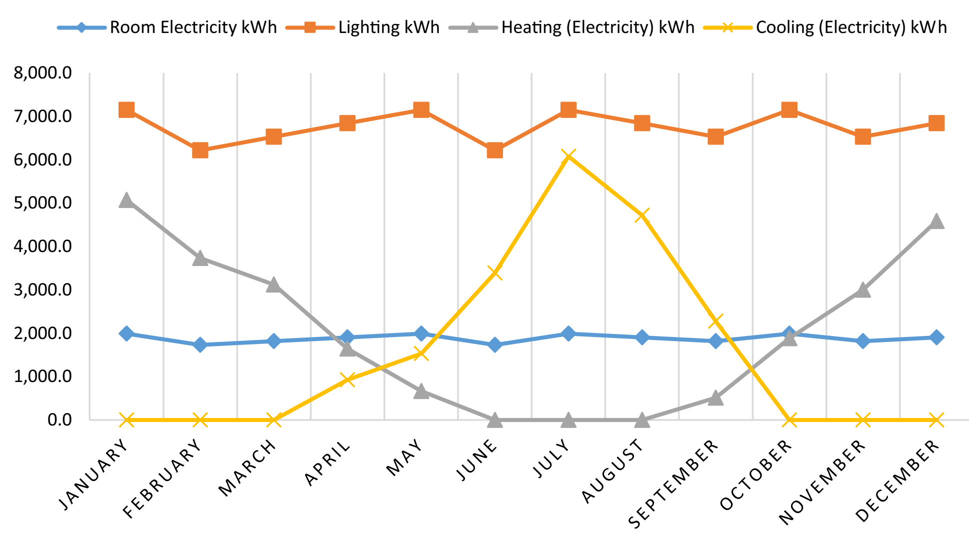

Fig. 17 Monthly energy consumption from case 5—efficient wall, roof, and glazing

Table 10 Comparative results for energy consumption per case scenario

Energy consumption (Kwh)					
Month	Case 1—base case	Case 2—efficient wall	Case 3—efficient roof	Case 4—efficient glazing	Case 5—efficient wall, roof, glazing
January	18,826	18,321	15,935	18,282	14,206
February	15,388	14,847	12,843	15,078	11,678
March	14,103	13,607	12,261	13,811	11,460
April	12,016	11,714	11,518	11,884	11,304
May	11,590	11,363	11,511	11,431	11,321
June	11,293	11,507	11,737	10,708	11,330
July	16,590	16,695	16,323	15,637	15,211
August	13,304	13,613	13,807	12,751	13,457
September	11,349	11,126	11,426	11,096	11,125
October	12,454	12,112	11,395	12,385	11,015
November	14,040	13,418	11,946	13,881	11,338
December	17,709	17,185	14,778	17,290	13,321
Total	168,662	165,508	155,481	164,235	146,766

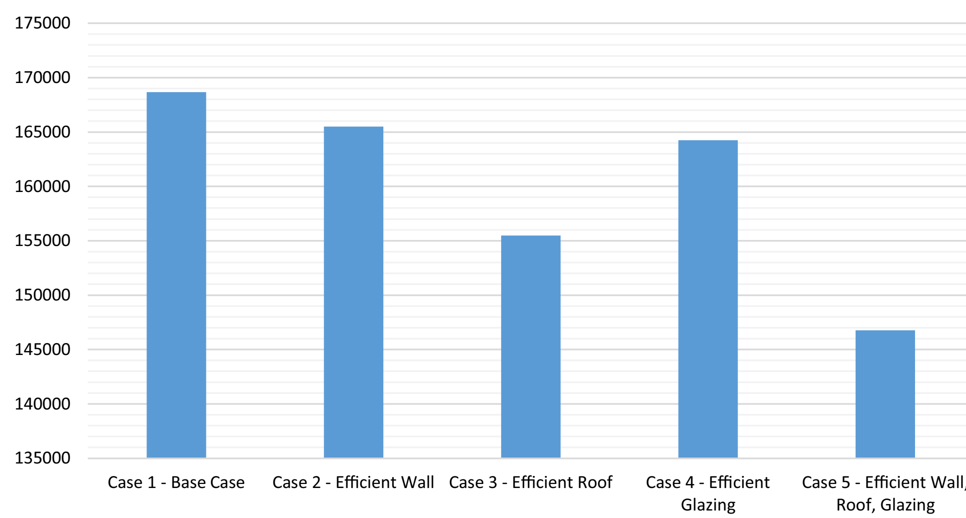

Fig. 18 Annually energy consumption (kWh) from cases scenario

Table 10 presents the annual comparative results for the total energy consumption per case scenario. Figure 18 shows the annual energy consumption for each case.

2.3.1.3 Heating energy demand Wuhai is located in a cold arid desert climate region. Therefore to maintain an appropriate temperature within the built environment, a heating system is required to complement heating energy demand. Table 11 shows the total heating energy demand per case scenario for the demonstration center throughout the year, while Fig. 19 presents the monthly variation according to each case.

2.3.2 Thermal comfort

Thermal comfort is most likely the most significant and readily defined IEQ factor. The human body strives to keep its temperature around 37 ℃. The temperature is maintained via heat exchange between the human body and the surrounding environment via convection, radiation, and evaporation [22].

2.3.2.1 Heat balance The heat balance consists of heat gains on one side and heat losses on the other. The heat losses consist of transmission, ventilation and infiltration, while the heat gains consist of solar loads, internal heat loads and heating systems. In this paper, only heat transmission causing heat to flow through the building envelope (wall, roof and windows) and solar load through the windows are addressed. To better understand the heat balance of the demonstration center, a simulation was carried out on the entire building with the main focus being on wall, roof and windows assemblies. The simulation was conducted throughout the year as presented in the figures below. Figure 20 shows the amount of heat loss through the wall when using

Table 11 Total heating demand per case scenario for the demonstration center

Heating demand (Kwh)—monthly					
Month	Case 1—base case	Case 2—efficient wall	Case 3—efficient roof	Case 4—efficient glazing	case 5—efficient wall, roof, glazing
January	9,603	9,186	6,711	9,058	5,071
February	7,367	6,903	4,822	7,057	3,734
March	5,681	5,266	3,839	5,389	3,119
April	2,910	2,656	2,007	2,818	1,644
May	1,315	1,081	838	1,335	661
June	0	0	0	0	0
July	0	0	0	0	0
August	0	0	0	0	0
September	1,265	1,012	722	1,272	509
October	3,231	2,977	2,172	3,162	1,880
November	5,618	5,077	3,524	5,459	2,997
December	8,886	8,447	5,956	8,467	4,583
Total	45,875	42,605	30,590	44,017	24,197

Fig. 19 Monthly energy consumption from cases scenario

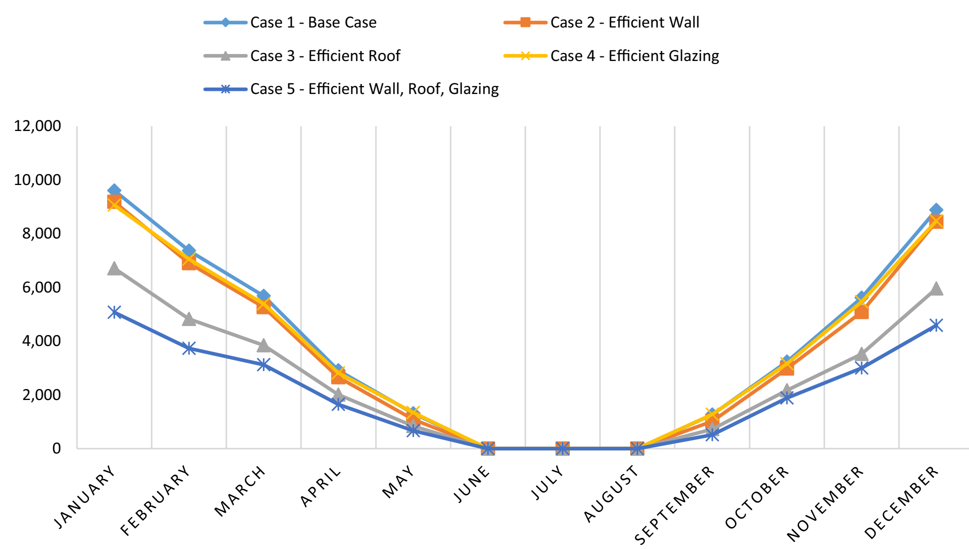

Fig. 20 Heat loss through the wall when using parameters form case 1, case 2 and case 5

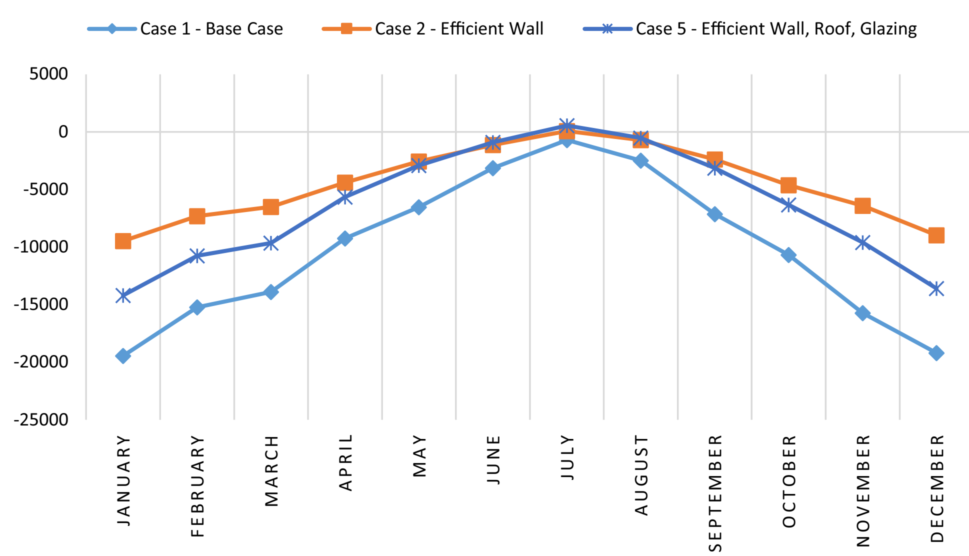

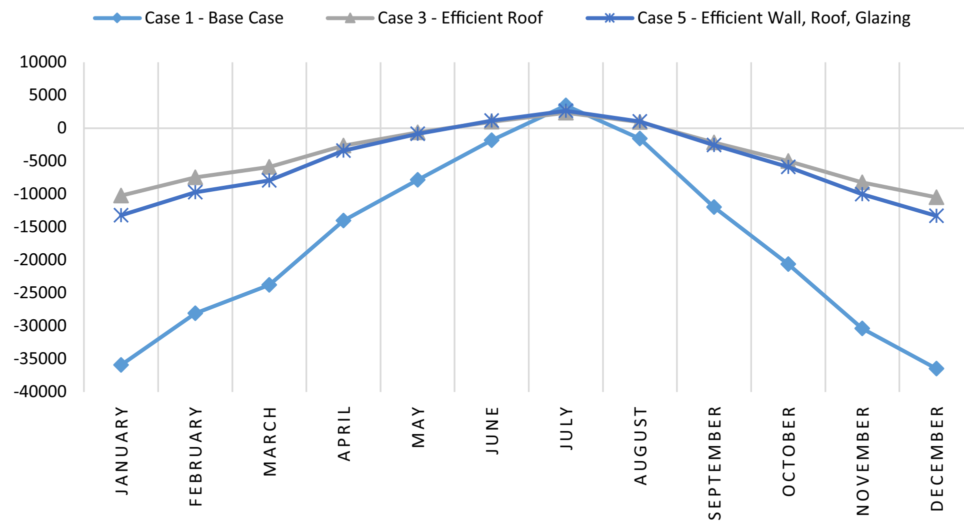

Fig. 21 Heat loss through the roof when using parameters from case 1, case 2 and case 5

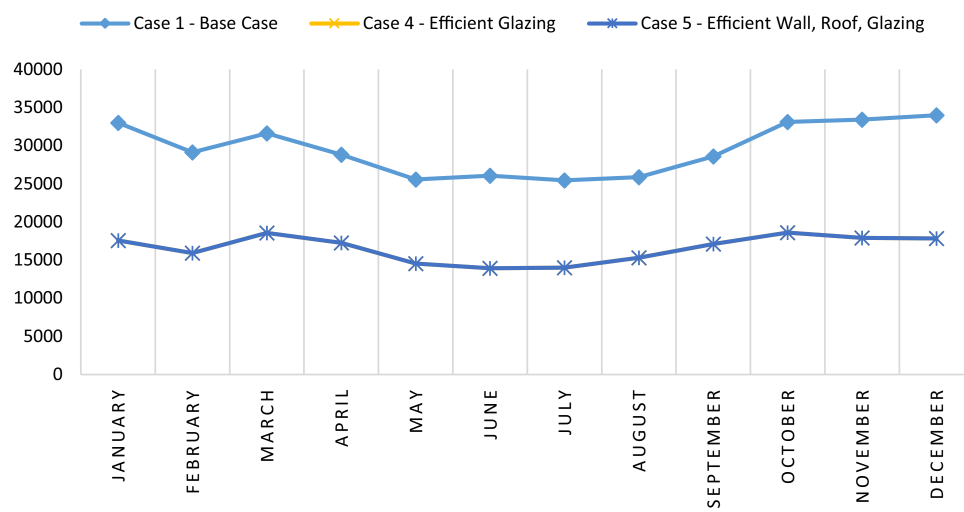

Fig. 22 Heat gain through glazing when using parameters from case 1, case 2 and case 5

parameters from case 1, case 2 and case 5, Fig. 21 shows the amount of heat loss through the roof when using parameters from case 1, case 2 and case 5 and Fig. 22 shows the amount of heat gain through windows when using parameters form case 1, case 2 and case 5.

2.3.2.2 Indoor temperature The indoor temperature denotes comfortable habitation for humans. Therefore, it remains a key factor in determining appropriate thermal comfort within a given space. To ensure that indoor temperature fluctuation is not affected by external conditions, parameters were set to the building envelope including wall, roof and windows, respectively represented as case 2, case 3 and case 4 while case 1 represents the base case model with standard parameters and case 5 represents a combination of case 1, 2 and 3. Table 12 presents the monthly indoor temperature for each case in comparison to the minimum and maximum comfortable temperature.

To easily analyze the different outputs, and determine which case scenario provide better conditions in terms of indoor temperature, case 2, case 3 and case 4 were compared to case 1 and case 5. Figure 23, Fig. 24 and Fig. 25 show the monthly indoor temperature level when using case 1, case 2, case 3, case 4 and case 5 as compared to minimum and maximum comfortable temperature.

3 Results and discussions

Building performance simulation (BPS) in the project was used to accurately evaluate the hypothetical building's performance on energy efficiency and thermal comfort, being the direct result of the implementation of passive design strategies and renewable technology use. The indoor simulation took into consideration the energy analysis and Indoor environment quality analysis under various scenarios cases

Table 12 Monthly indoor temperature per case scenario

Month	Case 1—base case	Case 2—efficient wall	Case 3—efficient roof	Case 4—efficient glazing	Case 5—efficient wall, roof, glazing	Min comfortable temperature	Max comfortable temperature
January	7.17	8.72	10.69	7.09	15.16	20.30	24.30
February	9.72	11.01	12.71	9.60	16.47	20.30	24.30
March	13.07	14.15	15.55	13.03	18.59	20.30	24.30
April	19.36	20.02	20.77	19.32	21.95	20.30	24.30
May	22.48	22.80	23.09	22.36	23.50	20.30	24.30
June	25.17	25.34	25.43	24.89	25.31	20.30	26.70
July	26.55	26.58	26.49	26.29	26.17	20.30	26.70
August	25.75	25.87	25.88	25.57	25.78	20.30	26.70
September	22.60	22.97	23.45	22.49	23.97	20.30	24.30
October	18.72	19.42	20.50	18.58	21.69	20.30	24.30
November	13.98	15.16	16.88	13.82	19.31	20.30	24.30
December	7.85	9.41	11.51	7.71	15.68	20.30	24.30

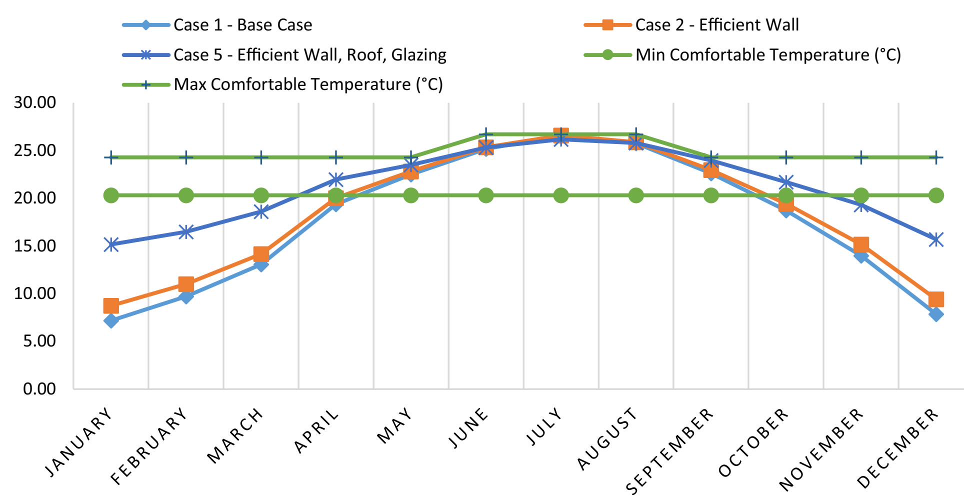

Fig. 23 Monthly indoor temperature level when using case 1, case 2 and case 5

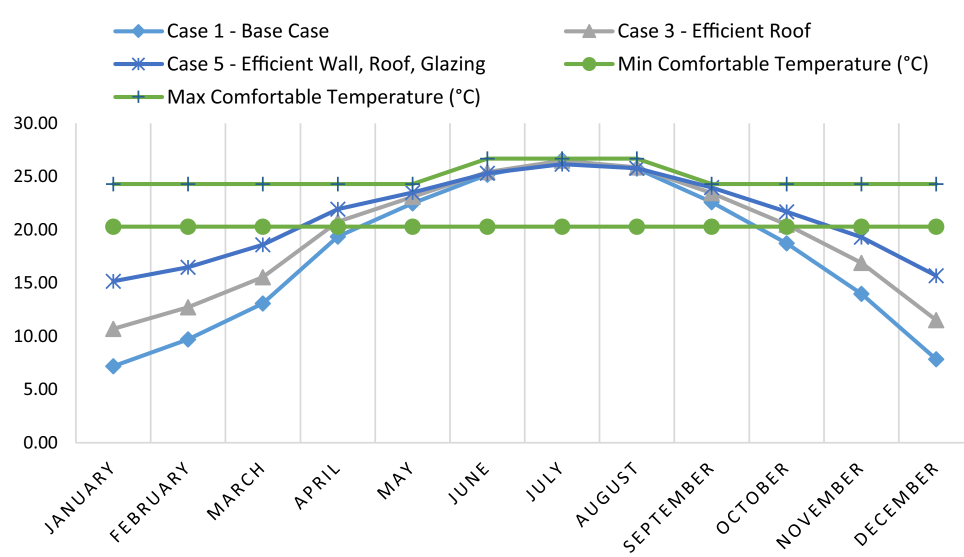

Fig. 24 Heat gain through glazing when using parameters from case 1, case 3 and case 5

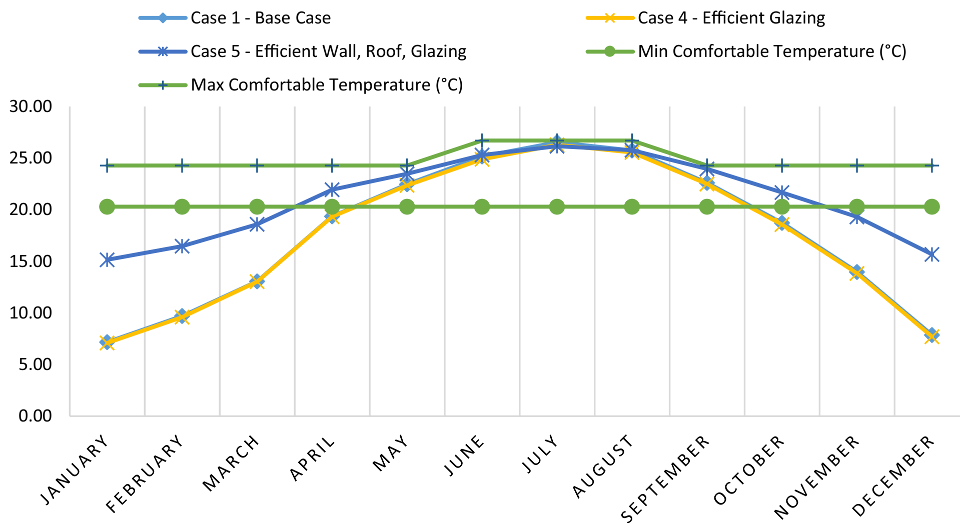

Fig. 25 Heat gain through glazing when using parameters from case 1, case 4 and case 5

from which parameters on wall, roof and glazing were adjusted. The results of these analyses will be discussed in the sections below.

3.1 Energy performance

3.1.1 Energy production

Energy analysis shows that the total energy generated by the entire site is about 983,904 kWh with a total PV area of 4122 m^2. It can be seen that the demonstration center has a total PV area of 963 m^2 with an annual energy generation of 214,414 kWh. Table 13 presents Total energy generation from of the entire site.

3.1.2 Energy consumption

With the input parameter set for the base scenario (case 1) throughout the year, the energy consumption is relatively high as compared to the remaining case scenarios. When parameters were set to case 2—efficient wall in Table 5, we observed a total energy consumption of 2% lower than that of the base case. When parameters were set to case 3—efficient roof in Table 6, we have an 8% reduction in the total energy consumption as compared to the base case. Furthermore, with the parameters in Table 7, case 4—efficient windows, the total reduction is only 3%. Finally, when the parameters were set to case 5—with the efficient wall, roof and window Table 8, a higher energy consumption reduction of 13% was observed. Table 14 below shows the total energy consumption and the percentage reduction as compared to the base case (case 1).

3.1.3 Heating energy demand

Besides the total energy consumption per case scenario, the total heating demand was also estimated separately. The results show that during the winter, there is an important

Table 13 Total energy generation from the entire agricultural demonstration park with emphasis on the demonstration part

Zoning	Spaces	PV Area (m^2)	Annual AC energy (kWh)
Building complex	Product supply center	317	70,483
	Demonstration center	963	214,414
Smart greenhouse	Smart greenhouse	1993	508,167
	PV pods	65	16,489
Energy plaza	Energy tree	264	58,761
	Energy tree outdoor area	92	20,476
	Plaza	51	11,426
	Plaza PV pods	5	1,186
	Reception	46	10,090
	Parking area	307	68,257
	Entrance PV pods	19	4,155

Table 14 Total energy consumption per case scenario and the percentage reduction as compared to the base case

Case scenario	Total energy consumption (kWh)	EPI (kWh/m^2)	Reduction compared to base case
Case 1—base case	168,662	44	–
Case 2—efficient wall	165,508	44	2%
Case 3—efficient roof	155,481	41	8%
Case 4—efficient glazing	164,235	43	3%
Case 5—efficient wall, roof, glazing	146,766	39	13%

Table 15 Total heating energy demand per case scenario and the percentage reduction as compared to the base case

Case scenario	Total energy heating demand (kWh)	EPI (kWh/m^2)	Reduction compared to base case
Case 1—base case	45,875	12	–
Case 2—efficient wall	42,605	11	75%
Case 3—efficient roof	30,590	8	82%
Case 4—efficient glazing	44,017	12	74%
Case 5—efficient wall, roof, glazing	24,197	6	86%

demand in heating. The base case heating energy demand is higher compared to other case scenarios as observed in Table 15. The maximum reduction of heating demand is achieved at 86% only when parameters are set to case 5 (Table 8) with the efficient wall, roof and windows.

The total energy produced by the PV system on the demonstration center is approximately around 214,414 kWh per year, meanwhile, the annual energy consumption achieved with the case 1—base case, case 2, case 3, case 4 and case 5 are respectively 168,662 kWh, 165,508 kWh, 155,481 kWh, 164,235 kWh and 146,766 kWh. It can be concluded that despite the significant reduction observed when parameters are set to case 5, which represents a total reduction of 13% as compared to case 1—base case, the demonstration center remains energy self-sufficient.

3.2 Thermal comfort

For this study, the results from thermal comfort will be limited to the heat balance and indoor temperature when the building is under different case scenarios.

3.2.1 Heat loss through the wall

The results from Fig. 20 were presented in Table 16 for better appreciation and a clear comparison of the case scenarios.

The results show that when parameters are set to case 2—efficient wall, the reduction in heat loss is up to 56% as compared with case 1, however, when parameters are set to case 5—efficient Wall, roof and windows, the reduction in heat loss is up to 38%. We can observe that in this particular scenario, the case 2—the efficient wall has a better reduction in heat loss.

3.2.2 Heat loss through the roof

The results from Fig. 21 were presented in Table 17 for better appreciation and a clear comparison of the case scenarios.

The results show that when parameters are set to case 3—efficient roof, the reduction in heat loss is up to 56% as compared with case 1, however, when parameters are set to case 5—efficient Wall, roof and windows, the reduction in heat loss is up to 77%. We can observe in this particular scenario, that case 3—the efficient roof has a better reduction in heat loss.

3.2.3 Heat gain through windows

The results from Fig. 22 were presented in Table 18 for better appreciation and a clear comparison of the case scenarios.

The results show that when parameters are set to case 4—efficient window, the reduction in heat gain is up to 44% as compared with case 1, however, when parameters are set to case 5—efficient Wall, roof and windows, the reduction in heat gain is also to 44%. We can observe in this particular scenario, that case 4—efficient and case 5—efficient wall, roof and window have the same heat gain reduction.

The results from heat balance show that significant reduction in heat loss through the wall is achieved when parameters

Table 16 Monthly heat loss through the wall for case 1, case 2 and case 5

Month	Heat Loss through Walls				
	Case 1—base case	Case 2—efficient wall	Case 3—efficient roof	Case 4—efficient glazing	Case 5—efficient wall, roof, glazing
January	−19,453.88	−9484.416	−30,003.78	−19,139.67	−14,194.58
February	−15,220.53	−7317.096	−24,393.46	−14,902.39	−10,744.36
March	−13,898.73	−6513.476	−24,329.63	−13,656.07	−9641.007
April	−9242.233	−4404.053	−16,824.59	−8854.251	−5643.557
May	−6539.576	−2566.929	−12,785.83	−6005.588	−2921.136
June	−3141.736	−1126.544	−8963.424	−2272.579	−918.3119
July	−705.5654	59.67284	−6329.438	48.12807	538.0616
August	−2480.41	−701.3948	−8145.367	−1863.836	−522.4208
September	−7146.729	−2386.591	−14,214.22	−6798.051	−3139.365
October	−10,674.31	−4617.074	−19,669.32	−10,188.73	−6331.411
November	−15,722.87	−6411.982	−26,101.54	−15,253.61	−9605.76
December	−19,182.37	−8981.195	−30,197.45	−18,732.55	−13,603.71
	−123,409	−54,451	−221,958	−117,619	−76,728
		56%			38%

Table 17 Monthly heat loss through the roof for case 1, case 3 and case 5

Month	Heat Loss through Roof				
	Case 1—base case	Case 2—efficient wall	Case 3—efficient roof	Case 4—efficient glazing	Case 5—efficient wall, roof, glazing
January	−35,924.84	−41,088.61	−10,237.13	−35,359.7	−13,235.45
February	−28,079.97	−31,903.88	−7482.38	−27,538.73	−9715.014
March	−23,787.45	−27,178.59	−5891.326	−23,366.46	−7934.457
April	−14,049.29	−16,108.86	−2665.943	−13,496.31	−3424.209
May	−7843.467	−8936.102	−658.5006	−7104.558	−891.5309
June	−1857.435	−2424.446	968.9775	−685.8856	1109.899
July	3434.16	3311.815	2330.002	4447.913	2604.509
August	−1576.526	−1982.422	901.9858	−739.8176	1002.055
September	−12,000.48	−13,288.85	−2191.135	−11,498.34	−2574.238
October	−20,644.23	−22,984.66	−5009.67	−19,947.06	−5906.029
November	−30,400.2	−33,954.73	−8242.222	−29,764.87	−10,025.55
December	−36,477.66	−41,594.97	−10,493.9	−35,778.72	−13,318.49
	−209,207		−48,671		−62,309
			77%		70%

are set case 2—efficient while significant reduction in heat loss through the roof is achieved when parameters are set case 3—efficient roof. Furthermore, a similar reduction in heat gain is achieved when parameters are set in case 4—efficient glazing and case 5—efficient wall, roof, and glazing.

3.2.4 Indoor temperature

The results for Monthly indoor temperature for each case in comparison to the minimum and maximum comfortable temperature are presented in Table 19.

The results show that when parameters are set to case 2—efficient wall, the monthly indoor temperature level within the comfort zone account for 5 months in the years, respectively May 22.8 ℃, June 25.17 ℃, July 26.55 ℃, August 25.75 ℃, and September 22.60 ℃. During the 7 remaining months, from October to April, the indoor temperature is below the comfort zone.

When parameters are set to case 3—efficient roof, the monthly indoor temperature level within the comfort zone account for 7 months in the years, respectively April 20.77 ℃, May 23.09 ℃, June 25.43 ℃, July 26.49 ℃, August

Table 18 Monthly heat gain through glazing for case 1, case 4 and case 5

Month	Heat gain/loss through glazing				
	Case 1—base case	Case 2—efficient wall	Case 3—efficient roof	Case 4—efficient glazing	Case 5—efficient wall, roof, glazing
January	32,995.88	32,945.84	32,995.88	17,545.48	17,540.68
February	29,101.76	29,053.89	29,101.76	15,914.46	15,909.83
March	31,613.02	31,557.2	31,613.02	18,553.04	18,547.55
April	28,817.26	28,763.47	28,817.26	17,268.54	17,263.19
May	25,572.75	25,522.78	25,572.75	14,536.92	14,531.97
June	26,049.91	26,000.48	26,049.91	13,926.19	13,921.32
July	25,427.48	25,378.17	25,427.48	14,006.33	14,001.48
August	25,870.77	25,822.37	25,870.77	15,312.35	15,307.54
September	28,562.77	28,511.08	28,562.77	17,111.85	17,106.73
October	33,098.64	33,042.54	33,098.64	18,590.12	18,584.66
November	33,419.71	33,367.36	33,419.71	17,887.59	17,882.56
December	33,967.35	33,916.66	33,967.35	17,830.83	17,825.97
	354,497			198,484	198,423
				44%	44%

Table 19 Monthly indoor temperature of case scenarios and minimum and maximum comfortable zone

Month	Case 1—base case	Case 2—efficient wall	Case 3—efficient roof	Case 4—efficient glazing	Case 5—efficient wall, roof, glazing	Min comfortable temperature	Max comfortable temperature
January	7.17	8.72	10.69	7.09	15.16	20.30	24.30
February	9.72	11.01	12.71	9.60	16.47	20.30	24.30
March	13.07	14.15	15.55	13.03	18.59	20.30	24.30
April	19.36	20.02	20.77	19.32	21.95	20.30	24.30
May	22.48	22.80	23.09	22.36	23.50	20.30	24.30
June	25.17	25.34	25.43	24.89	25.31	20.30	26.70
July	26.55	26.58	26.49	26.29	26.17	20.30	26.70
August	25.75	25.87	25.88	25.57	25.78	20.30	26.70
September	22.60	22.97	23.45	22.49	23.97	20.30	24.30
October	18.72	19.42	20.50	18.58	21.69	20.30	24.30
November	13.98	15.16	16.88	13.82	19.31	20.30	24.30
December	7.85	9.41	11.51	7.71	15.68	20.30	24.30

25.88 ℃, September 23.45 ℃ and October 20.5 ℃. During the 5 remaining months, from November to March, the indoor temperature is below the comfort zone.

The results show that when parameters are set to case 4—efficient glazing, the monthly indoor temperature level within the comfort zone account for 5 months in the years, respectively May 22.36 °C, June 24.89 ℃, July 26.26 ℃, August 25.57 ℃, and September 22.49 ℃. During the 7 remaining months, from October to April, the indoor temperature is below the comfort zone.

When parameters are set to case 3—efficient roof, the monthly indoor temperature level within the comfort zone account for 7 months in the years, respectively April 21.95 ℃, May 23.50 ℃, June 25.31 ℃, July 26.17 ℃, August 25.78 ℃, September 23.97 ℃ and October 21.69 ℃. During the 5 remaining months, from November to March, the indoor temperature is below the comfort zone.

However, when we compare case 2, case 3, case 4 and case 5 to the base case 1, the results show that case 5 provides more time within the comfort zone, which means there will be no energy demand for cooling or heating. Furthermore, from November to March, where indoor temperature level falls outside the comfort zone, there will be less energy demand to maintain the balance since, during those months, the temperature is not less than 15 ℃ as compared to case 3 which also provide the same time within the comfort zone. It can be concluded that with the use of passive design strategies and when parameters are set to case—5, thermal comfort can be achieved for 7 months in the year.

4 Limitations

It is strongly recognized that thermal comfort is a key parameter of IEQ, but because of its wide coverage, the author intends to report its comprehensive assessment in future studies. Therefore, the author acknowledges a major limitation in this study that could be addressed in future research. The limitation is that this study did not account for the Predicted Mean Vote (PMV) index and the Predicted Percentage Dissatisfied (PPD) index. While the PMV index predicts the mean comfort response of a larger group of people according to the ASHRAE thermal sensation scale, the PPD index is a quantitative measure of the thermal comfort of a group of people in any thermal environment. These two parameters would be considered and estimated in our subsequent studies.

5 Conclusion

The thermal comfort and the energy efficiency of a building and its components are inherently connected. In this project, the design team was confronted with the interplay between aesthetical, functional and economical aspects, which interact with both the energy and the thermal quality performance. In this study, the results of the assessment of the energy performance and thermal comfort of the demonstration center located in Wuhai, were presented. The assessment of energy performance and thermal comfort was achieved by implementing passive strategies and renewable technology into the design to meet the appropriate requirement to achieve indoor comfort and energy conservation. The energy performance factors measured were energy production, energy consumption and energy heating demand and the thermal comfort factors measured were heat balance and indoor air temperature. A comprehensive parametric analysis based on simulations was conducted with the goal of demonstrating how passive design solutions can increase indoor comfort while lowering energy consumption at a demonstration facility in Wuhai, located in a cold dry winters and hot summers region. The following are the findings of this study:

- By implementing proper passive design measures, it is possible to extend the non-heating and cooling seasons.
- The best passive design solutions share several characteristics, including a north to south orientation, a well-insulated building envelope, and a north to south orientation. In the best case scenario, these features result in a 13% reduction in energy consumption and an 86% reduction in heating demand when compared to the base case, and it maintains a comfortable indoor temperature for up to seven months a year with minimal maintenance
- Significant reduction in heat loss through the wall (56%) and heat loss through the roof (77%) are achieved when appropriate parameters are set. Furthermore, a similar reduction in heat gain (44%) is also achieved with the same parameters.
- Mechanical systems are still required to maintain a comfortable indoor atmosphere throughout the hottest and coldest periods of the year.

The evidence from this current assessment revealed that the quality of the indoor environment of the demonstration center is relatively good, pointing to the need for good implementation during the construction and appropriate maintenance culture during the operation phase. This is the first study of its kind on the passive design of a demonstration center in Wuhai, China's cold winter region.

Acknowledgements The authors would like to thank all research team members for their support and valuable comments that helped improve the paper.

Funding The authors have not disclosed any funding.

Declarations

Conflict of interest The authors declare that they have no competing interests.

References

1. Tanveer A, Anwer MA, Umar M (2021) The impact of environmental sustainability and financial resources utilization on firm financial performance: the mediating role of leadership styles. Ann Soc Sci Perspect. 2(2):389–407
2. Yao R, Steemers K, Li B (2006) Introduction to sustainable urban and architectural design. China Architectur and Building Press, pp 1–272
3. Olgyay V (2015) Design with climate: bioclimatic approach to architectural regionalism-new and expanded. Princeton University Press, Princeton
4. Zhu X et al (2014) Energy performance of a new Yaodong dwelling, in the Loess Plateau of China. Energy Build 70:159–166
5. Du X, Bokel R, van den Dobbelsteen A (2014) Building microclimate and summer thermal comfort in free-running buildings with diverse spaces: a Chinese vernacular house case. Build Environ 82:215–227
6. Yao R et al (2018) The effect of passive measures on thermal comfort and energy conservation. A case study of the hot summer and cold winter climate in the Yangtze River region. J Build Eng 15:298–310

7. Bebbington J, Unerman J (2018) Achieving the United Nations Sustainable Development Goals: an enabling role for accounting research. Account, Audit Account J
8. Lamb WF et al (2019) Learning about urban climate solutions from case studies. Nat Clim Chang 9(4):279–287
9. Bellia L et al (2021) On the interaction between lighting and thermal comfort: an integrated approach to IEQ. Energy Build 231:110570
10. Taveres-Cachat E et al (2019) Responsive building envelope concepts in zero emission neighborhoods and smart cities-a roadmap to implementation. Build Environ 149:446–457
11. Raziei T (2017) Köppen-Geiger climate classification of Iran and investigation of its changes during 20th century. J Earth Space Phys 43(2):419–439
12. Peel MC, Finlayson BL, McMahon TA (2007) Updated world map of the Köppen-Geiger climate classification. Hydrol Earth Syst Sci 11(5):1633–1644
13. Stevanović S (2013) Optimization of passive solar design strategies: a review. Renew Sustain Energy Rev 25:177–196
14. Quesada G et al (2012) A comprehensive review of solar facades. Opaque solar facades. Renew Sustain Energy Rev 16(5):2820–2832
15. Zahiri S, Altan H (2016) The effect of passive design strategies on thermal performance of female secondary school buildings during warm season in a hot and dry climate. Front Built Environ 2:3
16. Yovanof GS, Hazapis GN (2009) An architectural framework and enabling wireless technologies for digital cities & intelligent urban environments. Wireless Pers Commun 49(3):445–463
17. Paravantis JA, Kontoulis N (2020) Energy security and renewable energy: a geopolitical perspective, in renewable energy-resources, challenges and applications. IntechOpen, pp 3–18
18. Foster R, et al. (2003) Utilizing photovoltaics to support distance education in the state of Chihuahua, Mexico. In proceedings of the solar conference. American solar energy society; American institute of architects, pp 48–93
19. Chandel S, Naik MN, Chandel R (2017) Review of performance studies of direct coupled photovoltaic water pumping systems and case study. Renew Sustain Energy Rev 76:163–175
20. Llorens D (2018) Which direction should solar panels face. Solar Power Rocks,
21. Gevorkian P (2008) Solar power in building design: the engineer's complete design resource. McGraw-Hill Education, New York
22. Standard A Standard 55-2010 (2010) Thermal environmental conditions for human occupancy. American society of heating, refrigerating and air conditioning engineers. http://arco-hvac.ir/wp-content/uploads/2015/11/ASHRAE-55-2010.pdf. Accessed 3 Aug 2022